Available online at www.sciencedirect.com
ScienceDirect
Journal of Environmental Sciences 2011, 23(3) 412–418
JOURNAL OF ENVIRONMENTAL SCIENCES
ISSN 1001-0742
CN 11-2629/X
www.jesc.ac.cn

Characterization of condensed phase nitric acid particles formed in the gas phase

Long Jia[1,2], Yongfu Xu[1,*]

1. State Key Laboratory of Atmospheric Boundary Layer Physics and Atmospheric Chemistry, Institute of Atmospheric Physics, Chinese Academy of Sciences, Beijing 100029, China. E-mail: Jialong@mail.iap.ac.cn
2. Graduate University of Chinese Academy of Sciences, Beijing 100049, China

Received 25 April 2010; revised 21 June 2010; accepted 24 June 2010

Abstract

The formation of nitric acid hydrates has been observed in a chamber during the dark reaction of NO_2 with O_3 in the presence of air. The size of condensed phase nitric acid was measured to be 40–100 nm and 20–65 nm at relative humidity (RH) $\leqslant$ 5% and RH = 67% under our experimental conditions, respectively. The nitric acid particles were collected on the glass fiber membrane and their chemical compositions were analyzed by infrared spectrum. The main components of nitric acid hydrates in particles are $HNO_3{\cdot}3H_2O$ and $NO_3^-{\cdot}xH_2O$ ($x \geqslant 4$) at low RH, whereas at high RH $HNO_3{\cdot}H_2O$, $HNO_3{\cdot}2H_2O$, $HNO_3{\cdot}3H_2O$ and $NO_3^-{\cdot}xH_2O$ ($x \geqslant 4$) all exist in the condensed phase. At high RH $HNO_3{\cdot}xH_2O$ ($x \leqslant 3$) collected on the glass fiber membrane is greatly increased, while $NO_3^-{\cdot}xH_2O$ ($x \geqslant 4$) decreased, compared with low RH. To the best of our knowledge, this is the first time to report that condensed phase nitric acid can be generated in the gas phase at room temperature.

Key words: nitric acid; particles; relative humidity; chamber

DOI: 10.1016/S1001-0742(10)60414-7

Citation: Jia L, Xu Y F, 2011. Characterization of condensed phase nitric acid particles formed in the gas phase. Journal of Environmental Sciences, 23(3): 412–418

Introduction

The hydrates of nitric acid are of great interest because of their roles in the formation of polar stratospheric clouds and acid rain, therefore there are many studies that reveal the properties of nitric acid hydrates in cold vapor (Tolbert and Middlebrook, 1990; Ritzhaupt and Devlin, 1991; Koehler et al., 1992; Tolbert et al., 1992; Hanson and Mauersberger, 1988; Worsnop et al., 1993; Barton et al., 1993). Some studies showed that hydration of nitric acid can also take place under normal atmospheric conditions. Lee et al. (1980) studied the gas-phase clustering equilibria of NO_2^- and NO_3^- with high-pressure mass spectrometry, and pointed out that gas-phase nitric acid can reversibly bind water molecules to form $HNO_3{\cdot}nH_2O$, where the value n is dependent on the atmospheric water concentration. Eatough et al. (1985) studied the collection of gas phase nitric acid by diffusion denuders and further proved that the species collected on the nylon denuders is actually $HNO_3{\cdot}nH_2O$. Ramazan et al. (2006) recently studied the heterogeneous reaction of NO_2 with H_2O on the glass surface and suggested that HNO_3 can react with H_2O to form nitric acid hydrates on the glass surface at a temperature of 296 K.

It is usually believed that gaseous HNO_3 can react to form secondary aerosols on the surfaces of or within existing aerosol particles, but it can hardly nucleate to form new particles under normal circumstances, because the vapor pressure of HNO_3 at 293 K is approximately 10^5 to 10^7 times higher than that of H_2SO_4 (Spurny, 2000). Hence, the results have not been reported about nitric acid particles born in the gas phase at room temperature and pressure.

The previous studies of the reaction of HNO_3 with water were mainly focused on low temperature or on the surfaces. If HNO_3 can particulate in the ambient air condition, there will be two obvious effects: (1) the influences of the hydrates of nitric acid on the ratio of VOC/NOx and on the ozone pollution in the photochemical reactions, and (2) the direct contribution to the nucleation of clouds and hazes.

The purpose of the present work was to characterize the nitric acid particles formed during the reaction of NO_2 with O_3 at room temperature and ambient air pressure. To the best of our knowledge, this is the first time to characterize size distribution of HNO_3 particles in the gas phase at room temperature.

* Corresponding author. E-mail: xyf@mail.iap.ac.cn

1 Experimental

The experiments were performed in a 100 L reactor made of 0.1 mm FEP Teflon film at a temperature range of 289–295 K with a total pressure of 1 atm. The details of the apparatus have been described by Xu et al. (2006). Gas phase HNO_3 was generated by the reaction of NO_2 with O_3 in the absence of irradiation. Before each experiment, the reactor was washed using N_2 (99.999%), until O_3 and NO*x* concentrations were under the detecting limit. After the residual gas was pumped out, the given volumes of 101 ppm NO_2, synthetic air and ca. 500 ppm O_3 were sequentially introduced into the reactor according to the chosen reactant concentrations. Then, the reactor was vigorously shaken to make the reactants mixed thoroughly, after which timing the reaction began. At the same time, the ozone concentration was monitored on line. Synthetic air was used as background gas. The fine particles in synthetic air were removed by an Teflon holder that contains a PTFE (polytetrafluoroethylene) fiber membrane (pore size 0.2 μm, Sartorius, Germany). During each experimental course, the temperature varied about ± 1 K. After each experiment the reactor was flushed using synthetic air for 10 hr with a 40 W blacklight lamp on.

The gas-phase species such as N_2O_5, HNO_3, NO*x* and O_3 were determined by a long path Fourier transform infrared spectrometer (LP-FT-IR, Nicolet iS10, Thermo Fisher Scientific Inc., USA), which includes a 33 m permanently aligned long path gas cell (PIKE Technologies, USA). NO*x* (NO, NO_2) was simultaneously monitored by a chemiluminescence analyzer (Model 42C, Thermo Fisher Scientific Inc., USA). O_3 was monitored with a UV photometric O_3 analyzer (Model 49C, Thermo Fisher Scientific Inc., USA). The formation and evolution of particles in the range of 13.5–645 nm were monitored using a scanning mobility particle sizer (TSI Model 3034: DMA Model 3081 and CPC Model 3775, TSI Inc., USA). The chemical composition of particles collected on the glass fiber membrane (pore size 0.45 μm, Staplex, USA) was analyzed by FT-IR.

Table 1 Initial conditions for experiments

Exp. No.	O_3 (ppb)	NO_2 (ppb)	NO (ppb)	RH (%)	Temp. (K)
#1	1960	1191	12	67	295
#2	2074	1246	12	⩽ 5	293
#3	6200	3150	20	⩽ 5	293
#4	5310	3040	10	⩽ 5	293
#5	9500	5520	30	⩽ 5	289
#6	11270	5230	20	90	289

RH: relative humidity.

2 Results and discussion

Table 1 presents the experimental conditions for the chamber experiments. The rate constants for the O_3 and NO_2 wall losses were obtained to be 4.0×10^{-6} and 2.41×10^{-6} sec^{-1} in the chamber, respectively (Jia et al., 2009). Experiments #1 and #2 were used to characterize the size distribution of nitric acid hydrate clusters under RH = 67% and RH < 5%, respectively; #3 and #4 were used to study the total nitrate products and gas phase nitrate; and #5 and #6 were used to determine the influences of RH on the condensed phase nitrate products.

2.1 Determination of gas phase nitric acid

Many studies (Spicer et al., 1982; Akimoto et al., 1980; Grosjean, 1985) pointed out that the "NO_2" reading of a chemiluminescent NO*x* analyzer includes gaseous HNO_3. With similar initial concentrations of O_3 and NO_2 in Experiments #1 and #2, after 20 min of reaction, the Model 42C detected that the "NO_2" concentration in Experiment #2 (RH ⩽ 5%) was over 580 ppb higher than that in Experiment #1 (RH = 67%) (Fig. 1), which suggests the important role of RH in the NO_2-O_3 system.

The gas-phase NO_2-O_3 system is well characterized and is included in all kinetic models, such as in MCM (the Master Chemical Mechanism) (Saunders et al., 2003). Thus, the gas-phase concentrations of reactants and products like NO_2 can be obtained by computer modeling. The theoretically calculated NO_2 concentrations are in good agreement with "NO_2" readings under the high RH condition (Fig. 1a). However, when RH is low (⩽ 5%),

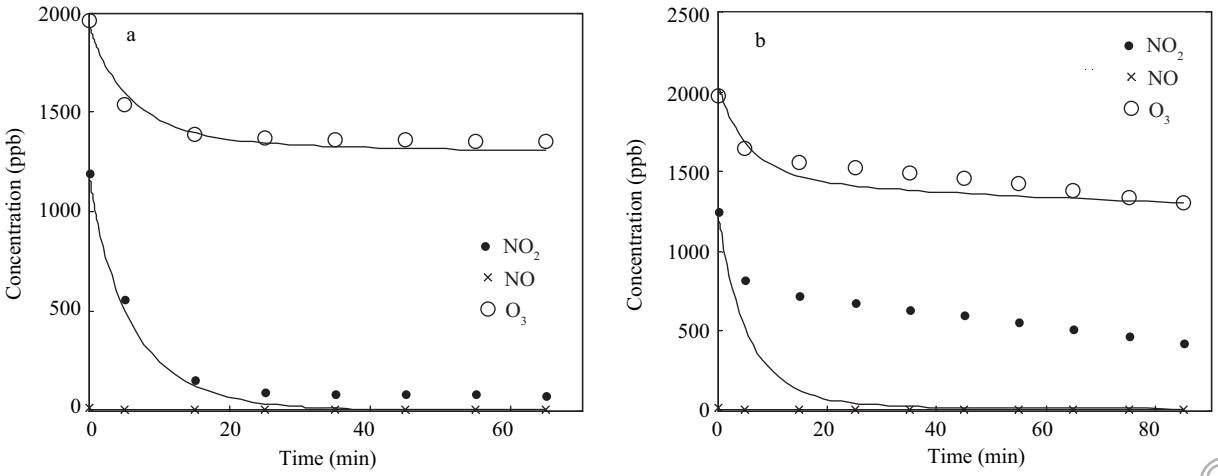

Fig. 1 Observed (symbols) and modeled (lines) concentration-time profiles of O_3 and NO*x* obtained in the NO_2-O_3 experiments (measured NO_2 include NO_2, HNO_3 and N_2O_5). (a) RH = 67% (Exp. #1); (b) RH ⩽ 5% (Exp. #2).

the "NO_2" reading is much higher than the calculated NO_2 (Fig. 1b). The possible reason is that gaseous nitric acid was converted into the condensed phase under the high RH condition and was filtered out by the Teflon membrane in the Model 42C inlet. Thus, the interference from gas-phase HNO_3 can be removed under the high RH condition. Several repeated experiments all confirmed the conclusion.

According to the model calculation of the NOx-O_3 system, after 60 min (in Experiments #1 and #2), NO_2 would be almost consumed (Fig. 1). Thus, we take 60 min as a reference time point. In Experiment #2 (Fig. 1b), after 60 min of the reaction over 558 ppb "NO_2" was still measured, which implied that there was over 558 ppb HNO_3 (or N_2O_5) in the gas phase and another 688 ppb nitric acid was formed in the condensed phase or on the chamber wall because of its combination with water. It can be considered that the condensed nitric acid particles were mainly formed because the wall loss of HNO_3 was ignorable. According to Bloss et al. (2005) who considered that the rate constant of the HNO_3 wall loss ranged from 4.1×10^{-5} sec^{-1} to 1.4×10^{-4} sec^{-1} in the NO_2-O_3 system, we estimate that the wall loss of HNO_3 was only 62 ppb at 60 min of reaction time. In Experiment #1 (Fig. 1a), the measured "NO_2" was only 80 ppb at 60 min, indicating that gaseous HNO_3 (or N_2O_5) was only 80 ppb, and that over 93% of nitric acid was probably converted into the particles.

2.2 Size distribution of nitric acid hydrate particles

To further ensure whether there was condensed phase nitric acid in the chamber, the size and number concentration of nitric acid particles with time was measured by DMA TSI Model 3081 with CPC TSI Model 3775. Results for both low and high RH conditions are shown in Fig. 2. Both lower panels show the variation of mean number concentrations with time. During the first 10 min, particles were seldom detected under both low and high RH conditions, because formed HNO_3 was very limited during this period. After 10 min, the number concentration began to accumulate and the particle size started to grow quickly. After 30 min both particle size and number concentration reached a relatively steady state. It can be seen that when RH is $\leqslant$ 5%, the particle size is in the range of 30 to 100 nm and the mean number concentration is 2060 cm^{-3}. When RH is 67%, the particle size is focused in the range of 20 to 60 nm and the mean number concentration is 820 cm^{-3}. The mean number concentration of nitric acid particles at high RH (67%) are decreased 60%, compared to that at low

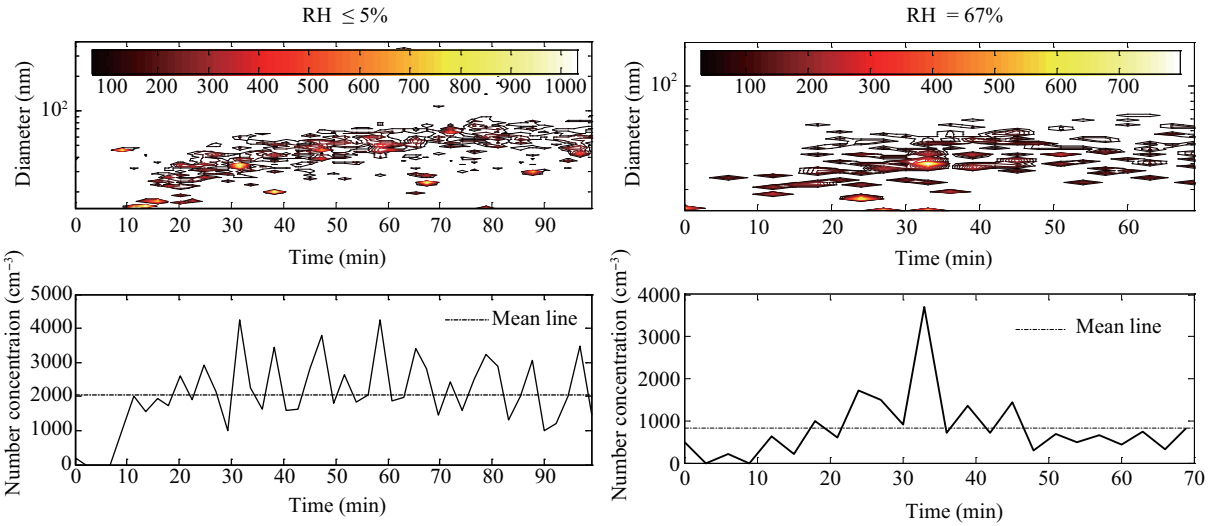

Fig. 2 Size and number concentration of nitric acid particles vs. reaction time.

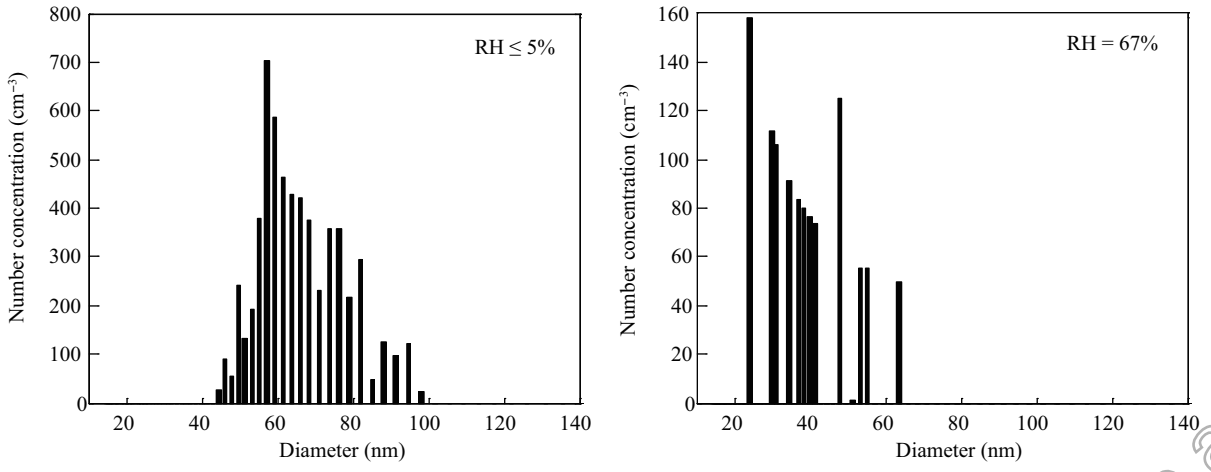

Fig. 3 Size distribution of nitric acid particles at 60 min of reaction time at RH $\leqslant$ 5% and RH = 67%.

RH ($\leqslant$ 5%), as shown in Fig. 2.

Figure 3 shows the size distribution of nitric acid particles, which is extracted from Fig. 2 at 60 min time point. This clearly indicates that RH changes the size distribution of particles. Under low RH of $\leqslant$5%, the size of nitric acid particles ranges from 40 to 100 nm, whereas under high RH of 67%, the measured particle size is mainly in a range of 20 to 65 nm. The largest number concentration appears to be at 58 nm at low RH, whereas it appears to be at 24 nm at high RH. Thus, we consider that high RH leads to the removal of nitric acid particles larger than 65 nm from the gas phase, and that high humidity is favorable for the small particles to be born and to grow.

2.3 Identification of total nitrate products

To determine the component of detected "NO_2" under low RH conditions, a glass fiber filter was used to sample total nitrate. The glass fiber filter that is relatively alkaline can approximate efficient total inorganic nitrate samplers and retain both particulate nitrate and HNO_3 with high efficiency under atmospheric conditions (Newman, 1993). Figure 4a shows the detected "NO_2" before and after the glass fiber filter for Experiment #3. The difference between "NO_2" readings before and after the glass fiber filter is 1204 ppb at 60 min. The detected "NO_2" is reduced by 76% after the glass fiber filter in the time period of 30–60 min. The reduced "NO_2" should come from gas phase HNO_3. This illustrates that gas phase HNO_3 accounts for 76% of total nitrogen-containing compounds in the gas phase. After the glass fiber filter, there are still 386 ppb "NO_2" remaining in the gas phase, which may come from gas phase N_2O_5.

The FT-IR spectrum of nitrate collected on the glass fiber membrane in the 1250–3650 cm^{-1} region is shown in Fig. 4b, in which the peak at near 3126 cm^{-1} is mainly nitric acid complexes with one or two water molecules. The spectrum (Fig. 4b) can be deconvoluted into six contributing peaks at 3380–3414, 3078, 2858, 2479, and 1422–1347 cm^{-1}, which is shown in Fig. 4b1, b2. According to Ramazan et al. (2006) and McCurdy et al. (2002), it is obvious that the peak at 3380–3414 cm^{-1} is H_2O. The peaks at 3080 and 2858 cm^{-1} can be assigned to $HNO_3{\cdot}H_2O$ and $HNO_3{\cdot}2H_2O$, respectively. The shoulder at 2479 cm^{-1} in Fig. 4b1 is assigned to $HNO_3{\cdot}3H_2O$. The absorption bands at 1417 and 1356 cm^{-1} are assigned to ν_3 asymmetric stretch of NO_3^- complexed to water ($NO_3^-{\cdot}xH_2O$) (x: 4–5) (Finlayson-Pitts et al., 2003). For this experiment, the spacing between the peaks of 1417 and 1356 is 61 cm^{-1}. In other experiments, the spacing can be 65 and 75 cm^{-1} at RH $\leqslant$ 5% and RH = 90%, respectively.

Experiment #4 was used to separate condensed phase HNO_3 and gas phase HNO_3. The combination of Teflon

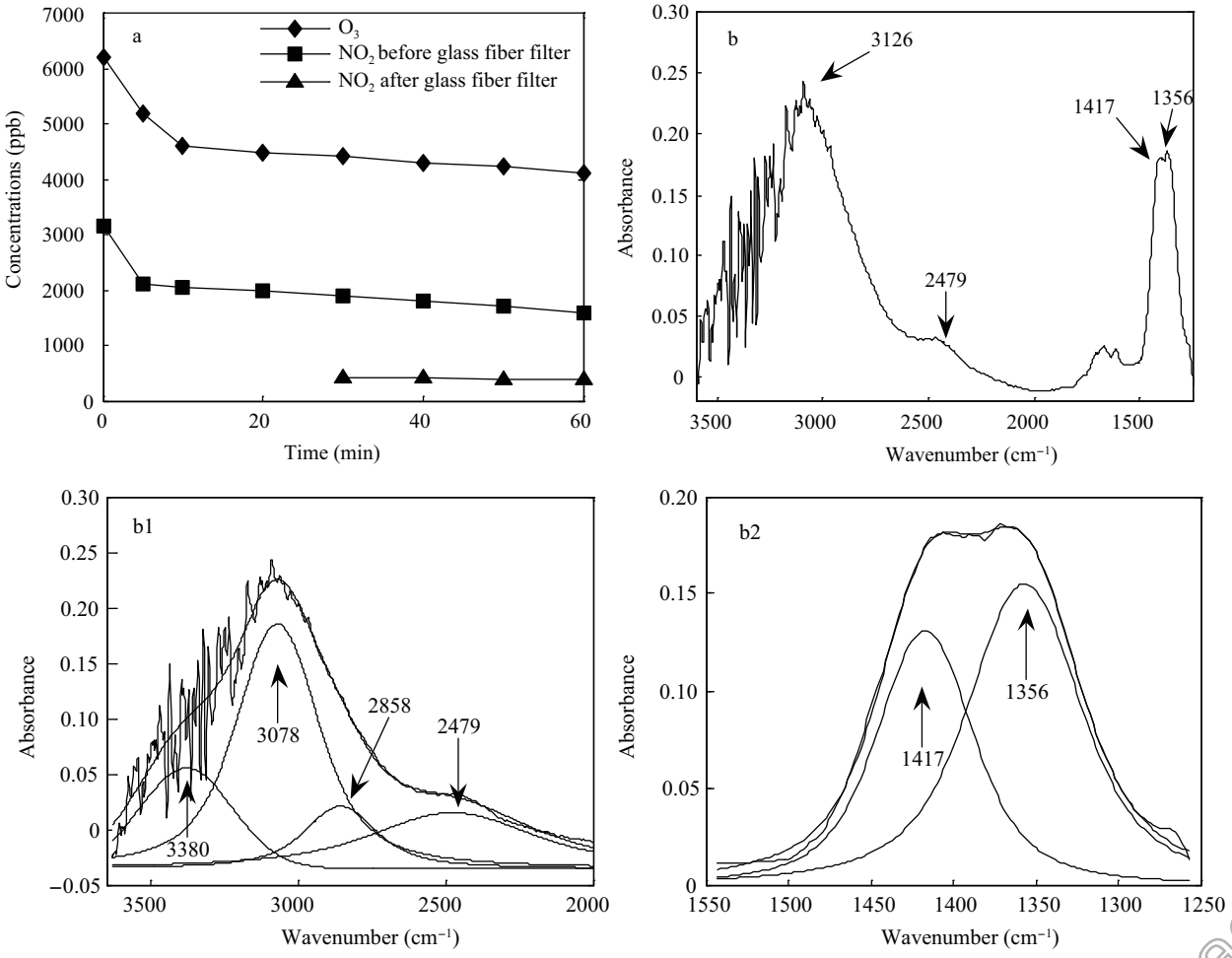

Fig. 4 Concentration-time profiles of NO_2 and O_3 for Exp. #3 before and after the glass fiber filter (a), and FT-IR spectrum of nitric acid hydrates collected on the glass fiber membrane from Exp. #3 (b).

and glass fiber filters in series was used to remove particles and determine gaseous HNO_3 (Mehlmann and Warneck, 1995). Gaseous HNO_3 collected on the glass fiber membrane was determined by FT-IR. When the RH is ⩽ 5%, the peaks (not shown) at both 3078 and 2858 cm^{-1} assigned to $HNO_3{\cdot}H_2O$ and $HNO_3{\cdot}2H_2O$ are almost as strong as those in Fig. 4b. The band at 2479 cm^{-1} assigned to $HNO_3{\cdot}3H_2O$ disappears. The peak heights at both 1356 cm^{-1} and 1417 cm^{-1} assigned to NO_3^- are about 14% of those in Fig. 4b. Although these weak peaks at both 1356 and 1417 cm^{-1} for Exp. #4 indicate that condensed HNO_3 ($NO_3^-{\cdot}xH_2O$) either may not be completely removed by the Teflon filter or is probably formed after the Teflon filter. It can be considered that $HNO_3{\cdot}3H_2O$ and $NO_3^-{\cdot}xH_2O$ do not exist in the gas phase. Therefore, we can conclude that $HNO_3{\cdot}H_2O$ and $HNO_3{\cdot}2H_2O$ mainly exist in the gas phase, and that $HNO_3{\cdot}3H_2O$ and $NO_3^-{\cdot}xH_2O$ are in the condensed phase at RH ≤ 5%.

2.4 Relative humidity impacts on nitric acid hydrates

To quantitatively study the influences of RH to nitric acid hydrates, the NO_2-O_3 system with high concentration was used. The nitric acid hydrates were collected with the glass fiber membrane at different RH conditions. Their spectrums and deconvolution are shown in Fig. 5. The quantity of nitric acid complexes is estimated from the Beer-Lambert law, as shown in Table 2.

Of these peaks, the peak at 3080 cm^{-1} assigned to $HNO_3{\cdot}H_2O$ is the largest contributor under both low and high RH conditions. The second contributor comes from the peak of $NO_3^-{\cdot}xH_2O$. Compared with the low RH condition (RH ⩽ 5%), the nitric acid hydrates of $HNO_3{\cdot}xH_2O$ (x ⩽ 3) are all increased, but $NO_3^-{\cdot}xH_2O$ is slightly decreased (1422–1347 cm^{-1}) under the high

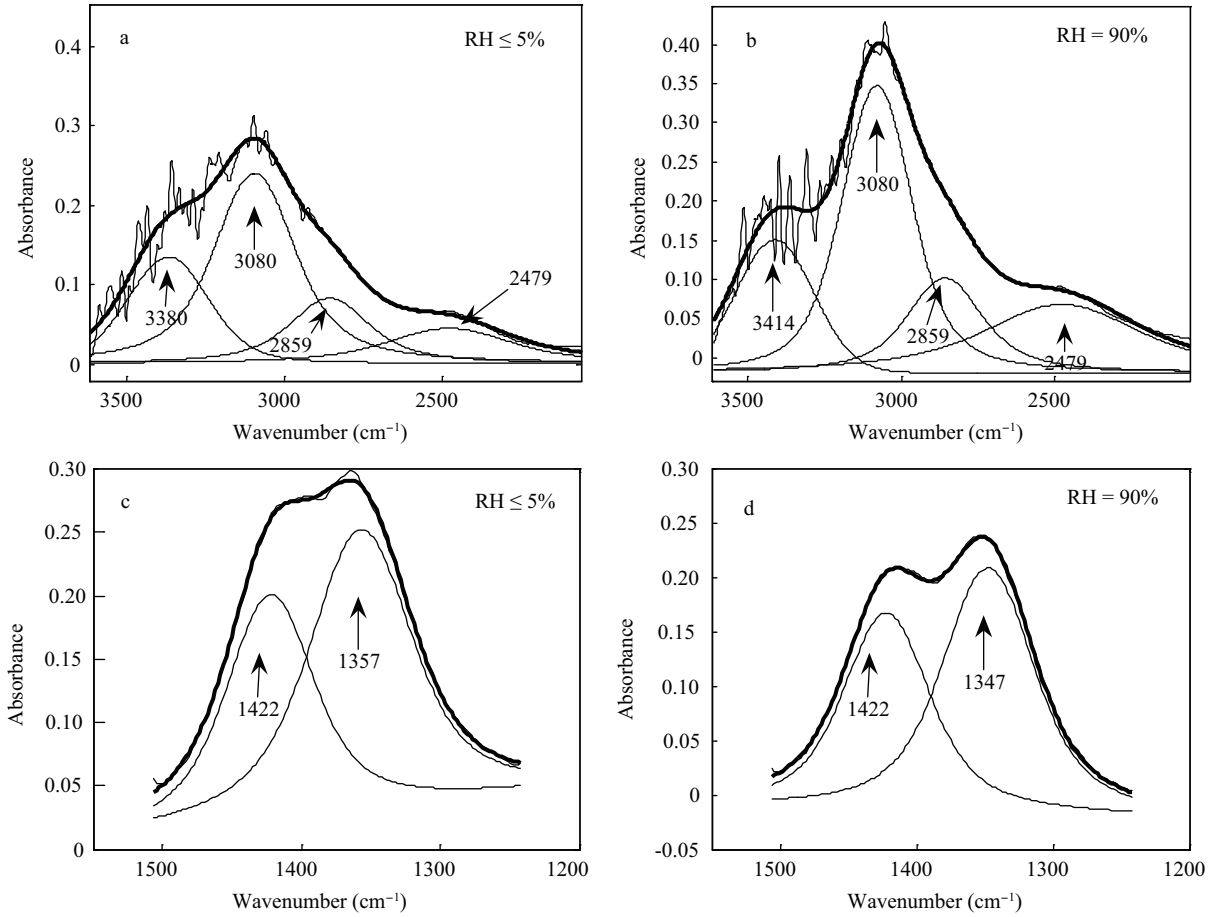

Fig. 5 Deconvolution of nitric acid hydrate absorbance bands (Exps. #5 and #6) collected on the glass fiber membrane. The irregular line represents the spectrum, the smooth lines indicate the individual peaks that make up the spectrum, and the solid bold line through the data is a summation of the individual contributions.

Table 2 Estimated concentrations of nitric acid complexes collected on the glass fiber membrane

Peak assignment	Band position (cm^{-1})	Band intensities (km/mol)[a]	RH ⩽ 5%		RH = 90%	
			Experimental integrated band intensity (cm^{-1})	Quantity ($\times10^5$ mol^{-1})	Experimental integrated band intensity (cm^{-1})	Quantity ($\times10^5$ mol^{-1})
$HNO_3{\cdot}H_2O$	3095	1121	100.2	0.089	127.2	0.113
$HNO_3{\cdot}2H_2O$	2860	1625	35.1	0.022	49.5	0.030
$HNO_3{\cdot}3H_2O$	2477	1896	29.5	0.016	77.7	0.041
$NO_3^-{\cdot}xH_2O$ (x: 4–5)	1347–1422	592	44.4	0.075	43.1	0.073

[a] The theoretical intensities reported by Ramazan et al. (2006).

RH condition (RH = 90%). This is in agreement with the change of the number concentrations of nitric acid particles under different RH conditions, including the increase of particles with the size of 20–40 nm and great decrease of particles larger than 65 nm.

The spacing between $NO_3^-\cdot xH_2O$ absorption peaks is 75 cm^{-1} at RH = 90%, whereas the spacing is 65 cm^{-1} at RH $\leqslant$ 5%, as shown in Fig. 5c, d. The measured spacing is different under different conditions, particularly at different matrix. Ritzhaupt and Devlin (1977) obtained the spacing of 150 and 65 cm^{-1} in an argon matrix containing 6% water and the matrix containing 100% water, respectively. Ramazan et al. (2006) observed a splitting of 93 cm^{-1} at RH = 50%. They pointed out that the spacing decreases as the amount of water associated with the nitrate ion increases. Theoretical calculation indicates the splitting of 101 cm^{-1} for nitrate associated with four water molecules and 62 cm^{-1} for the complex with five water molecules (Ritzhaupt and Devlin, 1977). Therefore, our results indicates that the H_2O number x in $NO_3^-\cdot xH_2O$ is reduced under the high RH condition. This conclusion is in agreement with the size distribution of nitric acid particles shown in Fig. 3, in which the larger particles containing more H_2O are removed under the high RH condition.

Figure 6 shows the changes of composition in nitrate particles for different RH conditions. When RH increases from 5% to 90%, the largest increase comes from $HNO_3\cdot xH_2O$ ($x \leqslant 3$), in which $HNO_3\cdot 3H_2O$ is increased by over 100%. We consider that as RH increases, the number x in $HNO_3\cdot xH_2O$ becomes great. When $x \geqslant 4$, $HNO_3\cdot xH_2O$ forms droplets and dissociates to form H_3O^+ and $NO_3^-\cdot xH_2O$. Compared to the change of particle size distribution in Fig. 3, when RH increases from 5% to 67%, the increased particles are mainly particles with the size of 20–40 nm. These particles should be $HNO_3\cdot xH_2O$ ($x \leqslant 3$). The reduced particles are mainly particles larger than 65 nm, which should be $NO_3^-\cdot xH_2O$. Ramazan et al. (2006) proposed a hypothesis that Reactions (1)–(4) might happen on the glass surfaces. Our experimental results indicate that these reactions can also take place in the gas phase.

$$HNO_3 + H_2O \longrightarrow HNO_3\cdot H_2O \quad (1)$$

$$HNO_3\cdot H_2O + H_2O \longrightarrow HNO_3\cdot 2H_2O \quad (2)$$

$$HNO_3\cdot 2H_2O + H_2O \longrightarrow HNO_3\cdot 3H_2O \quad (3)$$

$$HNO_3\cdot 3H_2O + yH_2O \longrightarrow H_3O^+ + NO_3^-\cdot xH_2O \quad (4)$$

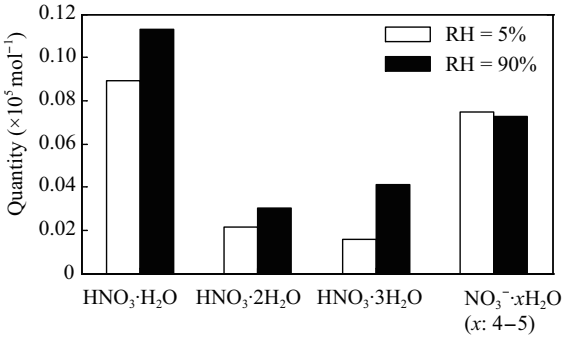

Fig. 6 Comparisons of estimated nitric acid complexes at different RH conditions.

3 Conclusions

The characterization of nitric acid hydrate particles formed from the dark reaction of NO_2 with O_3 has been investigated in the chamber under normal temperature and pressure. At low RH of ≤5%, $HNO_3\cdot H_2O$ and $HNO_3\cdot 2H_2O$ are mainly in the gas phase, while $HNO_3\cdot 3H_2O$ and $NO_3^-\cdot xH_2O$ ($x \geqslant 4$) are in the condensed phase. The size of condensed phase nitric acid hydrates were measured to be 40–100 nm. At high RH, $HNO_3\cdot H_2O$, $HNO_3\cdot 2H_2O$, $HNO_3\cdot 3H_2O$ and $NO_3^-\cdot xH_2O$ ($x\geqslant 4$) were all detected to be in the condensed phase, and the particle size was mainly in 20–65 nm. With the increase of RH, the quantity of $HNO_3\cdot H_2O$, $HNO_3\cdot 2H_2O$ and $HNO_3\cdot 3H_2O$ collected on the glass fiber membrane is greatly enhanced, whereas $NO_3^-\cdot xH_2O$ ($x \geqslant 4$) is slightly decreased. Compared with low RH of $\leqslant$ 5%, $HNO_3\cdot 3H_2O$ is increased by over 100% at high RH (90%). High RH is favorable for the small particles to be born and to grow, and can remove the larger particles containing more H_2O. To the best of our knowledge, our experiments are the first time to demonstrate that the formation of condensed nitric acid can take place in the gas phase at room temperature.

Acknowledgments

This work was supported by the Knowledge Innovation Program of the Chinese Academy of Sciences (No. KZCXZ-YW-Q02-03).

References

Akimoto H, Bandow H, Sakamaki F, Inoue G, Hoshino M, Okuda M, 1980. Photooxidation of the propylene-NOx-air system studied by long-path Fourier transform infrared spectrometry. *Environmental Science & Technology*, 14: 172–179.

Barton N, Rowland B, Devlin J P, 1993. Infrared spectra of large acid hydrate clusters: formation conditions of submicron particles of $HNO_3\cdot 2H_2O$ and $HNO_3\cdot 3H_2O$. *Journal of Physical Chemistry*, 97: 5848–5851.

Bloss C, Wagner V, Bonzanini A, Jenkin M E, Wirtz K, Martin-Reviejo M, Pilling M J, 2005. Evaluation of detailed aromatic mechanisms (MCMv3 and MCMv3.1) against environmental chamber data. *Atmospheric Chemistry and Physics*, 5: 623– 639.

Eatough D J, White V F, Hansen L D, Eatough N L, Ellis E C, 1985. Hydration of nitric acid and its collection in the atmosphere by diffusion denuders. *Analytical Chemistry*, 57: 743–740.

Finlayson-Pitts B J, Wingen L M, Sumner A L, Syomin D, Ramazan K A, 2003. The heterogeneous hydrolysis of NO_2 in laboratory systems and in outdoor and indoor atmospheres: An integrated mechanism. *Physical Chemistry Chemical Physics*, 5: 223–242.

Grosjean D, 1985. Wall loss of gaseous pollutants in outdoor Teflon chambers. *Environmental Science & Technology*, 19: 1059–1065.

Hanson D, Mauersberger K, 1988. Vapor pressures of HNO_3/H_2O solutions at low temperatures. *Journal of Physical Chemistry*, 92: 6167–6170.

Jia L, Xu Y F, Ge M F, Du L, Zhuang G S, 2009. Smog chamber

studies of ozone formation potentials for isopentane. *Chinese Science Bulliten*, 54: 4624–4632.

Koehler B G, Middlebrook A M, Tolbert M A, 1992. Characterization of model polar stratospheric cloud films using Fourier transform infrared spectroscopy and temperature programmed desorption. *Journal of Geophysical Research*, 97: 8065–8074.

Lee N, Keesee R G, Castleman A W Jr, 1980. The properties of clusters in the gas phase. IV. Complexes of H_2O and HNO*x* clustering on NO*x*. *Journal of Chemical Physics*, 72: 1089–1094.

McCurdy P R, Hess W P, Xantheas S S, 2002. Nitric acid-water complexes: theoretical calculations and comparison to experiment. *Journal of Physical Chemistry A*, 106(33): 7628–7635.

Mehlmann A, Warneck P, 1995. Atmospheric gaseous HNO_3, particulate nitrate, and aerosol size distributions of major ionic species at a rural site in western Germany. *Atmospheric Environment*, 29(17): 2359–2373.

Newman L, 1993. Measurement Challenges in Atmospheric Chemistry. American Chemical Society, Washington DC. 5–6.

Ramazan K A, Wingen L M, Miller Y, Chaban G M, Gerber R B, Xantheas S S et al., 2006. New experimental and theoretical approach to the heterogeneous hydrolysis of NO_2: key role of molecular nitric acid and its complexes. *Journal of Physical Chemistry A*, 110: 6886–6897.

Ritzhaupt G, Devlin J P, 1991. Infrared spectra of nitric and hydrochloric acid hydrate thin films. *Journal of Physical Chemistry*, 95: 90–95.

Ritzhaupt G, Devlin J P, 1977. Ionic vs. molecular nature of monomeric ammonium and hydronium nitrate. Infrared spectra of hydronium nitrate ($H_3O^+NO_3^-$) and ammonium nitrate ($NH_4^+NO_3^-$) solvated in argon matrices. *Journal of Physical Chemistry,* 81: 521–525.

Saunders S M, Jenkin M E, Derwent R G, 2003. Protocol for the development of the master chemical mechanism, MCMv3 (PartA): tropospheric degradation of non-aromatic volatile organic compounds. *Atmospheric Chemistry and Physics*, 3: 161–180.

Spicer C W, Howes Jr I E, Bishop T A, Arnold L H, Stevens R K, 1982. Nitric acid measurement methods: An intercomparison. *Atmosphere Environment*, 16: 1487–1500.

Spurny K R, 2000. Aerosol Chemical Processes in the Environment. Lewis Publishers, New York. 398.

Tolbert M A, Koehler B G, Middlebrook A M, 1992. Spectroscopic studies of model polar stratospheric cloud films. *Spectrochimica Acta*, 48A: 1303–1313.

Tolbert M A, Middlebrook A M, 1990. Fourier transform infrared studies of model polar stratospheric cloud surfaces: Growth and evaporation of ice and nitric acid/ice. *Journal of Geophysical Research*, 95: 22423–22431.

Worsnop D R, Fox L E, Zahniser M S, Wofsy S C, 1993. Vapor pressures of solid hydrates of nitric acid: Implications for polar stratospheric clouds. *Science*, 259: 71–74.

Xu Y F, Jia L, Ge M F, Du L, Wang G C, Wang D X, 2006. A kinetic study of the reaction of ozone with ethylene in a smog chamber under atmospheric conditions. *Chinese Science Bulletin*, 51: 2839–2843.